

Design and Holographic Field Reconstruction of Ultrasonic Lenses for Drug Delivery in non-Human Primates

Diana Andrés*, Alicia Carrión*, Nathalie Lamothe*, José A. Pineda-Pardo[†],
Noé Jiménez*, Francisco Camarena*

*Instituto de Instrumentación para Imagen Molecular, Consejo Superior de Investigaciones Científicas (CSIC) -
Universitat Politècnica de València (UPV), Spain

[†]HM CINAC, Fundación HM Hospitales de Madrid, Spain
Email: diaanbau@upv.es

Abstract—The aim of this work is to design and employ a large-aperture focused transducer with a holographic lens to selectively sonicate small deep-brain structures in non-human primates, such as the left post-commissural putamen, correcting skull aberrations and obtaining a good quality focal spot. Acoustic hologram was designed with time-reversal methods and numerical simulations with a k-space pseudospectral method. Its performance was experimentally evaluated with an ex-vivo macaque skull in water with direct measurements. To avoid undesired artefacts and retrieve the whole acoustic field, the focal region was also reconstructed by holographic projections of measurements taken at a 2D plane. Simulation, direct measurements and holographic projection results are in good agreement, with the focus lying into the therapeutical target location. We experimentally obtained that 38% of the target volume is sonicated with a pressure higher than half the focus maximum, getting more than 0.5 MPa rarefaction pressure. We present that holographic lenses coupled to large-aperture focused transducers allow for precise targeting of small deep brain structures at sufficient amplitudes to generate cavitation. This technology is presented as a low-cost system for preclinical localized drug delivery.

Index Terms—Ultrasound, acoustic holograms, holographic projection.

I. INTRODUCTION

Focused ultrasound is emerging as an alternative to existing medical techniques for several neurological disorders' treatment, mainly because it can be applied in a non-invasive manner. In addition, the non-ionising character of acoustic waves, even at high intensities, differentiate them from radiotherapy treatments for thermal ablation applications in the brain [1]. A promising application of therapeutic ultrasound is its use for drug delivery into the central nervous system. This is achieved by safely and reversibly opening the blood-brain barrier using a focused ultrasound beam inside the skull in combination with microbubbles previously injected with the drug into the bloodstream [2], [3]. In addition to this, there is ample evidence of neuronal stimulation and suppression achieved by focusing low-intensity ultrasound waves on specific brain structures [4], [5].

Despite the promise of this technology for transcranial therapy, the difficulty lies in the need for precise focusing of

the acoustic beam on the therapeutic target within the brain. In addition, the skull bones have a complex internal structure and high stiffness that causes ultrasound to propagate in a non-trivial way, undergoing reflection, refraction and attenuation, which affects the quality of the focus. A widely studied and successful solution is the use of magnetic resonance imaging (MRI)-guided phased arrays [6]. These systems have the disadvantage of requiring a large electronics system, which considerably increases their complexity and cost. A growing alternative are 3D printed holographic lenses [7], which coupled with single-element transducers are able to correct the aberrations introduced by the skull, generating a good quality acoustic focus adapted to the therapeutic target in the brain [8]. With the evolution of 3D printing techniques and the wide variety of materials available [9], this technology allows for great control of therapy at low cost and in a personalised way for each patient.

Multiple numerical studies on the performance of holographic lenses have been done, and the field generated by them in water and even through ex-vivo skull tissue have been assessed [10]–[14]. Experimental measurements reported in the literature evaluate the acoustic field generated by the transducer-lens system in specific planes or slices. However, the total volume and shape of the focus are not directly evaluated due to the amount of data and time cost involved.

In this work we study the design and performance of holographic lenses coupled to a focused transducer of large aperture and radius of curvature to treat small structures in the central nervous system of a non-human primate of the *macaca mulatta* species. The aim is to sonicate the left post-commissural putamen to achieve blood-brain barrier (BBB) opening in this small structure. Numerical simulations have been used to design and evaluate the performance of the optimal holographic lens. For experimental validation of the system, an ex-vivo macaque skull is available. Not only have direct measurements of the acoustic field been taken, but also the use of holographic projections has been proposed in order to recover the whole volume of the acoustic focus.

II. MATERIALS AND METHODS

A. Holographic lens design

In this study, a large-aperture focused transducer (OD = 100 mm diameter and $R = 140$ mm radius of curvature) with $f = 500$ kHz frequency and a central aperture of ID = 20 mm was used. This central orifice would allow the placement of a passive cavitation detector for location and monitoring of the BBB opening.

To generate the optimal acoustic hologram inside the skull, it is necessary to know the morphology and acoustic properties of the bone. Also, the hologram will be located according to the therapeutic target (left post-commissural putamen) segmentation. Bone shape and properties are extracted from CT images of the ex-vivo macaque skull. Its average density and sound speed values are $\rho_m = 1563 \text{ kg/m}^3$ and $c_m = 2191 \text{ m/s}$, obtained by converting X-ray attenuation values (Hounsfield Units) to acoustic impedance [15], [16]. Attenuation of the skull is set constant with value $\alpha_m = 9.6 \text{ dB/(cm MHz}^y\text{)}$, with $y = 1.1$, according to previously reported values [17]. Location and segmentation of the therapeutic target have been obtained from magnetic resonance images. The ex-vivo skull, medical images and target segmentation were provided by the HM CINAC hospital staff.

Time-reversal methods have been used to create the ultrasound hologram, and acoustic simulations have been performed using a pseudo-spectral method in the time domain implemented in the software *k-Wave* [18]. Following the procedure described in Ref. [8], a virtual source is located at the centre of the target position, in this case inside the left post-commissural putamen, and the phase information of the acoustic signals at the transducer's working frequency is captured at a surface in front of the transducer (holographic surface). This phase is complex-conjugated and used to create the holographic lens. The lens applies a phase shift to the acoustic waves depending on the material and height of each pixel, which is calculated in spherical coordinates to match the curvature of the transducer, with each pixel being perpendicular to the vibrating surface (as described in the supplementary material in Ref. [19]). This design allows subsequent 3D printing with stereolithography techniques for ex-vivo validation of the prototype. Values of density, sound speed and attenuation of the photopolymer used (Clear, Formlabs, USA) are $\rho_l = 1186 \text{ kg/m}^3$, $c_l = 2599 \text{ m/s}$ and $\alpha_l = 3.4 \text{ dB/(cm MHz}^y\text{)}$, experimentally measured in our laboratory.

B. Holographic projection

To validate the system, we first performed direct experimental measurements of the acoustic field at the focus. Then, we evaluated the field in a 2D plane 8 mm above the hologram focus (furthest from the transducer) which we called the holographic measurement plane (see Fig. 1). With this information and using holographic techniques we could reconstruct the entire 3D volume quickly, without the need to measure all acoustic signals point by point.

To perform the holographic projection, we time-reversed

and backward projected all the signals recorded in the 2D measurement plane, considering homogeneous propagation in water, without acoustic losses, so that the time symmetry of the wave equations is fulfilled. Dimensions of the holographic measurement plane must be large enough to capture the information of all the acoustic waves that conform the focus, with a resolution of at least $\lambda/2$ (in our case $\lambda/6$) to fully represent the field in the absence of evanescent waves, as in this case, since the plane is located more than a wavelength away from the source ($\lambda = 3 \text{ mm}$). These signals are then temporally inverted and windowed according to the arrival time and length of the transducer generated pulse. In this way we avoid the backprojection of reflections of the waves with the surface of the water and with the skull. When we propagate backwards these signals we reconstruct the entire acoustic field of the hologram.

C. Experimental setup

Experimental measurements were performed in degassed water at room temperature inside a tank with dimensions $40 \times 80 \times 60 \text{ cm}^3$ (height \times length \times width). The used transducer was made of a piezoelectric ceramic, with the physical dimensions described in Section 2. *Materials and methods*, mounted in a customized stainless steel housing. In order to locate and fix the skull relative to the lens, so that the experiment is reproducible and assure the same simulation conditions, we designed a 3D holder that adapts to the anatomy of the bone. The lens is coupled to the transducer with high temperature coupling gel (Sonotech Sono 600) to avoid its dissolution in water and to ensure a continuous coupling of the lens to the transducer. A schematic of the experimental system is presented in Fig. 1. The transducer was excited

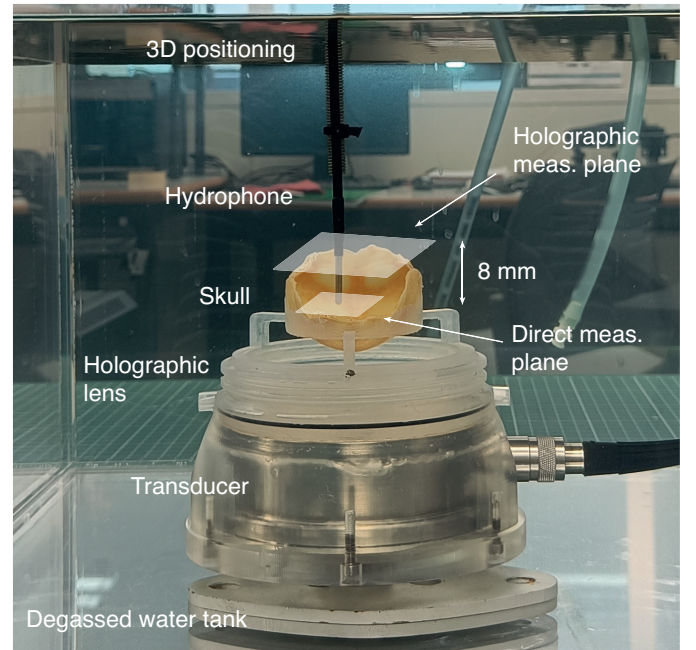


Fig. 1. Experimental setup for the transducer-lens system ex-vivo validation. Both holographic and direct measurement planes are schematically represented

with a 20-cycle sinusoidal pulse burst at 500 kHz with a signal generator (14-bit, 100 MS/s, model PXI-5412, National Instruments, USA) and amplified with a linear RF amplifier (ENI 1040L, 400 W, 55 dB, ENI, Rochester, NY, USA). The acoustic field was measured with a piezoelectric hydrophone (-225.5 dB re 1 V/ μ Pa at 1 MHz, model Y-104, Sonic Concepts, USA), calibrated from 40 kHz to 2 MHz, mounted on a 3D axis system (5 μ m resolution, PI Micos GmbH, Germany).

III. RESULTS

First, we obtained the simulated acoustic hologram field, considering the lens and all the experimental components (transducer, skull and holder). Size of the focus considering a pressure greater than half the maximum pressure (-3 dB) is $3 \times 3 \times 14$ mm³, with 55% of the focus volume lying in the target region. Numerically, 14% of the volume of the left post-commissural putamen (349 mm³) was sonicated. The XY and YZ planes evaluated at the pressure maximum location are shown in Figs. 2 a) and b), respectively.

Direct experimental measurements consisted of three 2D planes (XY, XZ and YZ) with dimensions 14×14 mm², 14×27 mm² and 14×27 mm², respectively, and spatial resolution of 0.5 mm in all directions, centred at the experimental pressure maximum (Figs. 2 c), d)). The size of the direct-measured holographic focus is $4.5 \times 4.5 \times 15.5$ mm³. In Fig. 3 we compare all three results in x, y and z lineal cuts through the experimental maximum.

The acoustic field obtained from the backward projection of the signals captured at the holographic measurement plane, of size 37×32 mm² and resolution of 0.5 mm, shows a

focus size of $4 \times 4 \times 14$ mm³. The holographic projection of the field shows that 40% of the volume of the focus falls in the therapeutic target region. The volume of left post-commissural putamen sonified is 38%. If we compare these values with those obtained directly in simulation, the volume of the therapeutic target treated is larger (38% experimental versus 14% obtained numerically), but the size of the focus is also larger. Holographic projection results in the same experimental XY and YZ planes are represented in Figs. 2 e), f), respectively.

With the use of holographic projection techniques to reconstruct the entire focal volume, only a measurement of a 2D plane was necessary (4736 signal measurements). The corresponding experimental time with our system was four hours, considering 3 seconds per measurement (time last for 15 acquisitions averaging and 3D positioning system movement). The hypothetical direct measurement of the entire volume with the same dimensions ($14 \times 14 \times 27$ mm³) and spatial resolution (0.5 mm), would consist of 42336 measurements, which would take 35.3 hours. It is important to note that if we wanted larger direct measurement volume, this would require additional experiments, whereas using the holographic projection method it can be enlarged only by further post-processing of the original data.

Direct measurements at the focal maximum were performed over a wide range of acoustic powers, obtaining pressure values above 0.5 MPa in water at 500 kHz, demonstrating that the transducer-lens system has enough power for blood-brain barrier opening in combination with a contrast agent [20].

IV. CONCLUSIONS

In this work we have demonstrated that the use of holographic lenses allows. On the one hand, to correct the aberrations introduced by the skull in the ultrasound propagation path, and on the other hand, to adapt the focus of a large aperture and radius of curvature transducer to small structures of interest inside the brain of a *macaca mulatta* primate. Experimental measurements verify the simulated shape and location of the acoustic holographic foci.

In addition, the holographic projection correctly reconstructs the focus, with very similar results to the direct experimental measurement in the same plane. We have demonstrated that this technique makes it possible to reconstruct the entire acoustic field around the focus and thus quantify its volume with a single experimental measurement, while avoiding artefacts that may appear due to the proximity of the hydrophone to the skull and, in addition, greatly reducing the time and resources needed to perform the characterization.

V. ACKNOWLEDGMENTS

This research has been supported by the Ministerio Español de Ciencia e Innovación and the Ministerio de Universidades through grants Juan de la Cierva – Incorporación IJC2018-037897-I, Juan de la Cierva – Formación FJC2019-040453-I, Formación de Profesorado Universitario FPU19/00601, and the national plan Retos PID2019-111436RB-C22, by the

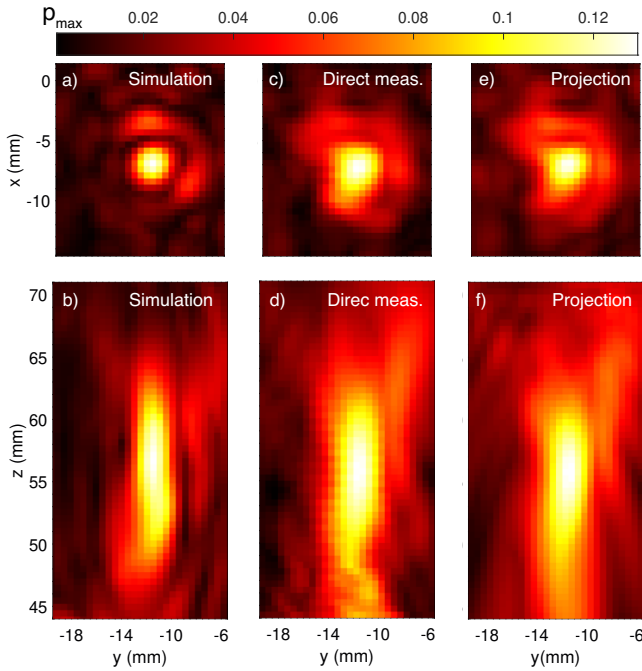


Fig. 2. a,c,e) XY-planes at the focus maximum for a) simulation, b) direct measurement and e) holographic projection. b,d,f) YZ-planes at the focus maximum for b) simulation, d) direct measurement and f) holographic projection.

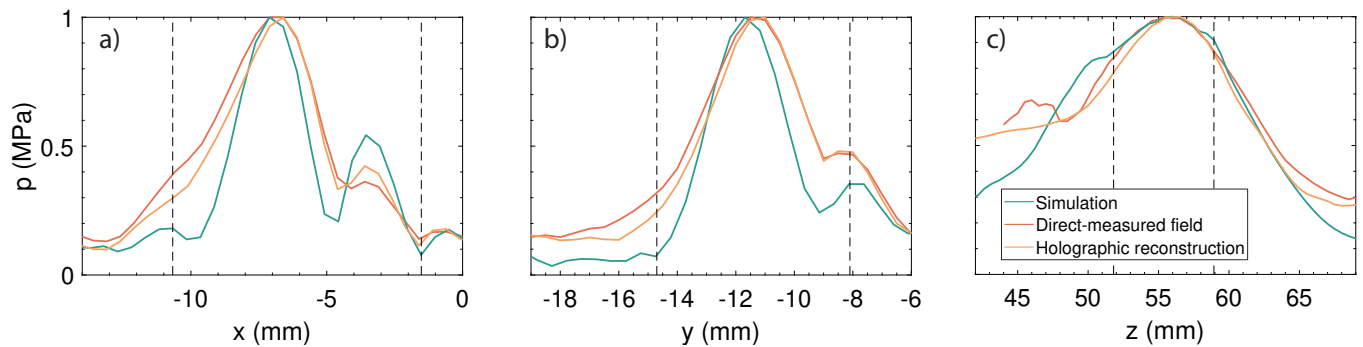


Fig. 3. Lineal cuts at the experimental focus maximum for the simulation, direct measurement and holographic projection results at the a) x-axis, b) y-axis and c) z-axis.

Agencia Valenciana de la Innovació through grants IN-NVA2/2022/11, and by Generalitat Valenciana through grants FDEGENT/2019/004, the project of Ayudas Emergentes CIGE/2021/175, the program Prometeo CIPROM/2021/003 and the program Equipamiento e Infraestructuras FEDER 2021-22 IDIFEDER/2021/004.

REFERENCES

- [1] A. Franzini, S. Moosa, D. Servello, I. Small, F. DiMeco, Z. Xu, W. J. Elias, A. Franzini, and F. Prada, "Ablative brain surgery: an overview," *International Journal of Hyperthermia*, vol. 36, no. 2, pp. 64–80, 2019.
- [2] N. McDannold, C. D. Arvanitis, N. Vykhodtseva, and M. S. Livingstone, "Temporary disruption of the blood–brain barrier by use of ultrasound and microbubbles: safety and efficacy evaluation in rhesus macaques," *Cancer research*, vol. 72, no. 14, pp. 3652–3663, 2012.
- [3] A. N. Pouliopoulos, S.-Y. Wu, M. T. Burgess, M. E. Karakatsani, H. A. Kamimura, and E. E. Konofagou, "A clinical system for non-invasive blood–brain barrier opening using a neuronavigation-guided single-element focused ultrasound transducer," *Ultrasound in medicine & biology*, vol. 46, no. 1, pp. 73–89, 2020.
- [4] W. Legon, T. F. Sato, A. Opitz, J. Mueller, A. Barbour, A. Williams, and W. J. Tyler, "Transcranial focused ultrasound modulates the activity of primary somatosensory cortex in humans," *Nature neuroscience*, vol. 17, no. 2, pp. 322–329, 2014.
- [5] W. Legon, L. Ai, P. Bansal, and J. K. Mueller, "Neuromodulation with single-element transcranial focused ultrasound in human thalamus," *Human brain mapping*, vol. 39, no. 5, pp. 1995–2006, 2018.
- [6] A. Abrahao, Y. Meng, M. Llinas, Y. Huang, C. Hamani, T. Mainprize, I. Aubert, C. Heyn, S. E. Black, K. Hynynen, *et al.*, "First-in-human trial of blood–brain barrier opening in amyotrophic lateral sclerosis using mr-guided focused ultrasound," *Nature communications*, vol. 10, no. 1, pp. 1–9, 2019.
- [7] K. Melde, A. G. Mark, T. Qiu, and P. Fischer, "Holograms for acoustics," *Nature*, vol. 537, no. 7621, pp. 518–522, 2016.
- [8] S. Jiménez-Gambín, N. Jiménez, J. M. Benlloch, and F. Camarena, "Holograms to focus arbitrary ultrasonic fields through the skull," *Physical Review Applied*, vol. 12, no. 1, p. 014016, 2019.
- [9] A. Antoniou, N. Evripidou, M. Giannakou, G. Constantinides, and C. Damianou, "Acoustical properties of 3d printed thermoplastics," *The Journal of the Acoustical Society of America*, vol. 149, no. 4, pp. 2854–2864, 2021.
- [10] G. Maimbourg, A. Houdouin, T. Defieux, M. Tanter, and J.-F. Aubry, "3d-printed adaptive acoustic lens as a disruptive technology for transcranial ultrasound therapy using single-element transducers," *Physics in Medicine & Biology*, vol. 63, no. 2, p. 025026, 2018.
- [11] S. Jiménez-Gambín, N. Jiménez, and F. Camarena, "Transcranial focusing of ultrasonic vortices by acoustic holograms," *Physical Review Applied*, vol. 14, no. 5, p. 054070, 2020.
- [12] G. Maimbourg, A. Houdouin, T. Defieux, M. Tanter, and J.-F. Aubry, "Steering capabilities of an acoustic lens for transcranial therapy: numerical and experimental studies," *IEEE transactions on biomedical engineering*, vol. 67, no. 1, pp. 27–37, 2019.
- [13] S. Jiménez-Gambín, N. Jiménez, A. N. Pouliopoulos, J. M. Benlloch, E. E. Konofagou, and F. Camarena, "Acoustic holograms for bilateral blood–brain barrier opening in a mouse model," *IEEE Transactions on Biomedical Engineering*, vol. 69, no. 4, pp. 1359–1368, 2021.
- [14] D. Andrés, N. Jiménez, J. M. Benlloch, and F. Camarena, "Numerical study of acoustic holograms for deep-brain targeting through the temporal bone window," *Ultrasound in Medicine & Biology*, vol. 48, no. 5, pp. 872–886, 2022.
- [15] U. Schneider, E. Pedroni, and A. Lomax, "The calibration of ct hounsfield units for radiotherapy treatment planning," *Physics in Medicine & Biology*, vol. 41, no. 1, p. 111, 1996.
- [16] T. D. Mast, "Empirical relationships between acoustic parameters in human soft tissues," *Acoustics Research Letters Online*, vol. 1, no. 2, pp. 37–42, 2000.
- [17] R. S. Cobbold, *Foundations of biomedical ultrasound*. Oxford university press, 2006.
- [18] B. E. Treeby and B. T. Cox, "k-wave: Matlab toolbox for the simulation and reconstruction of photoacoustic wave fields," *Journal of biomedical optics*, vol. 15, no. 2, p. 021314, 2010.
- [19] D. Andrés, J. Vappou, N. Jiménez, and F. Camarena, "Thermal holographic patterns for ultrasound hyperthermia," *Applied Physics Letters*, vol. 120, no. 8, p. 084102, 2022.
- [20] N. McDannold, N. Vykhodtseva, and K. Hynynen, "Use of ultrasound pulses combined with definity for targeted blood–brain barrier disruption: a feasibility study," *Ultrasound in medicine & biology*, vol. 33, no. 4, pp. 584–590, 2007.